

Precision Spectroscopy of High- L , $n = 10$ Rydberg Helium: An Improved Test of Relativistic, Radiative, and Retardation Effects

E. A. Hessels, F. J. Deck, P. W. Arcuni,^(a) and S. R. Lundeen

Department of Physics, University of Notre Dame, Notre Dame, Indiana 46556

(Received 25 July 1990)

We report improved measurements of the $10G-H$, $10H-I$, $10I-K$, and $10K-L$ fine-structure intervals in atomic helium, obtained using fast-beam microwave-optical techniques. The measurement uncertainty is less than 1 kHz in each of sixteen measured intervals. The existence of very precise calculations of the nonrelativistic contributions to these intervals allows the measurements to be used to test relativistic and QED effects directly, and to confirm the predicted contributions from "retardation" forces due to two-photon exchange to better than 10%.

PACS numbers: 32.30.Bv, 31.30.Jv

Since the suggestion in 1978 by Kelsey and Spruch that precise measurements of fine-structure intervals in high- L helium Rydberg states could reveal the influence of "retardation" or "Casimir" forces,¹ considerable effort, both experimental and theoretical, has been devoted to this goal. New theoretical techniques have been developed for calculating the nonrelativistic eigenvalues and relativistic corrections of these states,^{2,3} and for evaluating the predicted retardation effects for specific states.⁴⁻⁶ Experimental results of increasing precision have come from fast-beam microwave-optical experiments.⁷⁻¹⁰ We report here a new set of measurements which determine the mean energy intervals separating $n = 10$, $L = 4-8$ states of helium with a precision of about ± 0.4 kHz, which is sufficient to clearly resolve the predicted retardation effects. We find agreement with these predictions to the few-percent level, but only when several other relativistic and radiative corrections are fully accounted for.

The experimental method has been described in some detail elsewhere.^{9,10} A beam of fast helium Rydberg states is prepared by charge exchange from a fast ion beam ($v/c = 0.00266$), and specific $n = 10$ Rydberg levels are efficiently detected by resonant excitation to a higher- n state followed by Stark ionization and collection of the resulting ions. The primary spectroscopy is carried out in a section of transmission line in which the helium beam interacts with a traveling-wave microwave field which induces resonant electric dipole transitions between different fine-structure levels. To achieve selective population and detection of $L > 5$ levels, which are

unresolved by the laser, auxiliary rf regions (driven incoherently) are added before and after the main spectroscopy region to invert the populations of selected levels. Table I summarizes the mode of operation for each of the four transition groups studied in this experiment. The auxiliary rf transitions (rf1 and rf2 in Table I) partially resolve the magnetic fine structure (MFS) of the levels under study, and allow the selection of an individual MFS component of the resonance.¹⁰ Figure 1 illustrates, for instance, the four measured resonance line shapes for the $10I-10K$ transition.

The main microwave interaction region is an improved version of the region described elsewhere.⁹ The new region is longer (3 m) to give a narrower resonance line-

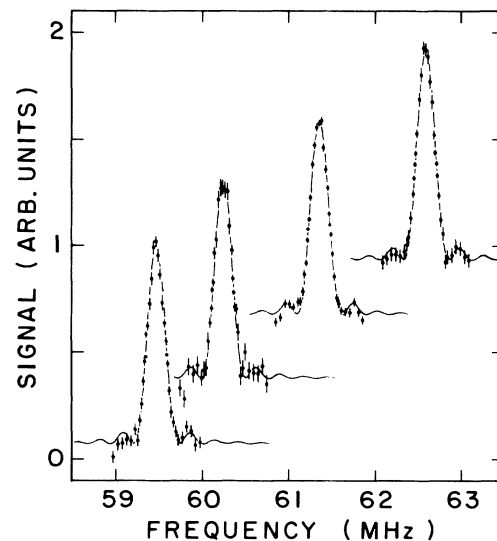


FIG. 1. Observed resonance line shapes for the four MFS components of the $10I-K$ transition, corresponding to transitions between corresponding levels of the $10I$ and $10K$ systems. Only a single peak occurs in each spectrum. The smooth curves are fits with the expected two-level line shape, broadened by time of flight. For these observations, the helium beam and rf traveling wave are copropagating, so the resonances are Doppler-shifted upwards.

TABLE I. Operating conditions used for the observations of four transition groups among $n = 10$ helium fine-structure levels. Unless explicitly stated, the levels referred to are in $n = 10$.

Transition	Laser 1	rf1	rf2	Laser 2
$G-H$	$G-30H$	$H-30I$
$H-I$	$H-30I$	$H-30I$
$I-K$	$H-30I$	$H-I$	$H-I$	$H-30I$
$K-L$	$H-30I$	$H-K$	$H-K$	$H-30I$

width (250 kHz), has a smaller reflection coefficient ($\Gamma \leq 0.03$) to reduce the distorting effects of the traveling wave reflected from the exit port, and is entirely constructed of copper to reduce dc electric fields which could result from contact-potential differences between the inner and outer conductors. It is enclosed in a magnetic shield to reduce the Earth's magnetic field to ≤ 0.003 G, and its outer surface is heated to approximately 60°C to reduce stray fields due to surface charging.¹⁰

The most troublesome systematic effect in this measurement is associated with the presence of small stray electric fields within the main interaction region which cause Stark shifts of the measured resonances at rates of -13 , -15 , -8 , and $+32$ MHz/(V/cm)² for the G - H , H - I , I - K , and K - L transitions, respectively. In the present measurement, these fields have been reduced to about 5 mV/cm rms, and have been carefully measured (to ± 1 mV/cm) by observing the 28^3D - $28F$ transition,^{10,11} which Stark shifts at a rate of -3800 MHz/(V/cm)², and the two-photon $10K$ - $10M$ transition,⁹ which shifts at a rate of 154 MHz/(V/cm)².

Resonance line shapes for each of the sixteen transitions were measured for each direction of microwave propagation and for each physical orientation of the main microwave interaction region. Each line was fitted by a symmetric resonance function to determine the best line center for that configuration, and then the results from the four configurations were averaged to give a result free of first-order Doppler shifts and reflected-wave shifts.⁹ This entire procedure was repeated three times, for a total of about 300 h of data collection. To obtain the final results, a number of small systematic corrections were applied to account for (a) time dilation, (b) Stark shifts from stray fields, (c) overlap of neighboring resonances, and (d) ac shifts due to 330-K blackbody radiation.¹² The total corrections are quite small. Aside from time dilation, the total systematic corrections are a factor of 10 smaller than in previous measurements.¹⁰ Table II shows the net correction for each of the sixteen measured intervals, along with the final corrected results. From these individual transition energies, the energy difference between the statistically weighted mean energy for each L state can be computed using Eq. (6) of Ref. 10. This mean energy interval is also shown in Table II. The final measurement precision in the mean energy intervals is about 0.3% of the natural linewidths¹³ for the G - H , H - I , and I - K intervals, and somewhat larger for the K - L interval. When available, the most recent previous measurements for each interval are also shown in Table II. A comparison reveals satisfactory agreement with previous results for the H - I , I - K , and K - L mean intervals, but a significant discrepancy (2.6σ) for the G - H interval, which may indicate that systematic corrections were underestimated in the earlier measurement.

There are a number of theoretical calculations which

TABLE II. Measured frequencies of sixteen specific fine-structure transitions. All results are in MHz with 1-standard-deviation errors given in parentheses. $\Delta v_{\text{sys}}^{\text{tot}}$ is the total systematic correction which was applied to each interval. v_0 is the final result of the present measurements. The mean energy intervals, which are calculated from the measurements as described in the text, are also shown. The last column shows the most recent previous measurements (Refs. 9 and 10), where available.

Transition	$\Delta v_{\text{sys}}^{\text{tot}}$	v_0	v_0^{prev}
$+G_4 - +H_5$	0.0018(3)	486.8622(8)	486.8657(17)
$^3G_3 - ^3H_4$	0.0022(3)	488.6677(10)	488.6720(20)
$^3G_5 - ^3H_6$	0.0019(3)	491.9668(7)	491.9705(14)
$-G_4 - -H_5$	0.0020(3)	<u>495.5571(8)</u>	<u>495.5605(17)</u>
$\bar{G} - \bar{H}$		491.0087(5)	491.0124(13)
$+H_5 - +I_6$	0.0006(1)	154.6689(4)	...
$^3H_4 - ^3I_5$	0.0007(1)	155.8155(5)	...
$^3H_6 - ^3I_7$	0.0008(1)	157.6299(4)	...
$-H_5 - -I_6$	0.0009(1)	<u>159.6490(4)</u>	...
$\bar{H} - \bar{I}$		157.0535(2)	157.0518(26)
$+I_6 - +K_7$	-0.0001(2)	59.3131(4)	...
$^3I_5 - ^3K_6$	0.0006(2)	60.0876(5)	...
$^3I_7 - ^3K_8$	0.0003(1)	61.1966(3)	...
$-I_6 - -K_7$	0.0003(1)	<u>62.4320(4)</u>	...
$\bar{I} - \bar{K}$		60.8165(2)	60.8156(18)
$+K_7 - +L_8$	-0.0011(3)	26.1678(6)	...
$^3K_6 - ^3L_7$	-0.0002(5)	26.7085(8)	...
$^3K_8 - ^3L_9$	-0.0010(3)	27.4385(6)	...
$-K_7 - -L_8$	-0.0008(3)	<u>28.2488(6)</u>	...
$\bar{K} - \bar{L}$		27.1750(5)	27.1837(63)

are tested by these measurements. They represent two contrasting views of the Rydberg atom: (1) the long-range interaction picture (LRI) in which the atom is treated as a single electron interacting with the He^+ -ion core, and (2) the standard atomic theory (SAT) picture in which it is treated as just another two-electron atom. The most complete calculation is in the SAT approach by Drake,¹⁴ who obtains extremely precise two-electron wave functions variationally and then calculates relativistic corrections, including the spin structure, by taking expectation values of the Breit-Pauli Hamiltonian and additional operators which account for both one- and two-electron radiative corrections. Less complete calculations in the LRI picture treat the spin structure,^{8,15,16} the mean energy intervals,² and the two-photon exchange contribution to the mean interval which contains the retardation effect.⁴⁻⁶

Calculations of the spin structure can be tested with a precision of 10^{-4} by noting the offset of individual MFS components from the mean energy interval. The SAT predictions of Drake^{13,14} show complete agreement with experiment. Those of Idrees and Fischer¹⁷ agree for $L > 4$ states. The LRI predictions^{8,15,16} also agree with experiment for $L > 4$ states and give a prescription for predicting spin structure in other high- L states.¹⁸

TABLE III. Nonrelativistic separations (including finite-mass corrections) of mean energies between high- L helium Rydberg levels, as calculated by Drake (Ref. 14) and Drachman (Ref. 2). The last column shows the difference between the experimentally measured mean energy difference and the most precise nonrelativistic calculation. All results are in MHz.

Interval	ΔE_{nr} (Drake)	ΔE_{nr} (Drachman)	$\Delta E_{\text{expt}} - \Delta E_{nr}$
$G-H$	484.0604	484.0424(5210)	6.9483(5)
$H-I$	152.1947	152.1927(97)	4.8588(2)
$I-K$	57.2388	57.2392(4)	3.5777(2)
$K-L$...	24.4347(2)	2.7403(5)

The measurements also test predictions of the mean energy intervals. These are dominated by the nonrelativistic contributions which have been calculated both in the SAT^{3,14} and in the LRI² approaches. As illustrated in Table III, the predicted nonrelativistic intervals from both approaches are in full agreement where they can be compared, although the SAT results are generally much more precise. The difference between the measured mean intervals (Table II) and the most precise nonrelativistic results is shown in the last column of Table III. These residuals represent the total of all relativistic, radiative, and retardation effects, and are determined in this way with a precision of better than 10^{-4} .

In the LRI picture, these residuals are accounted for by several specific effects: (1) the " p^4 " relativistic term in the electron's kinetic energy with appropriate finite-nuclear-mass corrections,^{19,20} (2) relativistic corrections to the adiabatic polarizabilities of He^+ ,² and (3) the hydrogenic expectation value of the "two-photon exchange potential" V_{ret} .²¹ As illustrated in Table IV, the subtotal of these three effects is in significant disagreement with experiment. However, another effect, easily included in the LRI picture, although apparently overlooked to date, is the change in the core electron's Lamb shift due to polarization of the core by the Rydberg electron. Using the long-range approximation of Drake,³ this effect contributes

$$\Delta \mathcal{L}_c = \frac{31}{128} \langle (r/a_0)^{-4} \rangle_{nL} \mathcal{L}(\text{He}^+ 1S). \quad (1)$$

With the addition of this term, the LRI picture agrees with experiment to the kHz level for the highest- L intervals, confirming the predicted contribution from $\langle V_{\text{ret}} \rangle$ to about 10%. However, remaining discrepancies suggest that other relativistic corrections remain to be accounted for in this approach.

In the SAT approach of Drake,¹⁴ the total relativistic contribution is composed of the spin-averaged expectation value of the Breit-Pauli Hamiltonian corrected for finite nuclear mass (denoted ΔE_{rel} in Table IV), and the one- and two-electron radiative shifts ($L1$ and $L2$). The subtotal of these is that SAT prediction, and is quite close to experiment. As has been discussed by Drake³

TABLE IV. Comparison between experimentally measured relativistic contribution to high- L helium fine-structure intervals and the predictions of two theoretical models. Experimental values (Expt.) are from Table III. All values are in MHz.

Term	$G-H$	$H-I$	$I-K$	$K-L$
Long-range interactions picture				
" p^4 "	7.0773	4.8997	3.5931	2.7477
" $\Delta \alpha_{\text{rel}}$ "	-0.1095	-0.0339	-0.0127	-0.0054
$\langle V_{\text{ret}} \rangle$	-0.0422	-0.0126	-0.0045	-0.0018
Subtotal	6.9256	4.8532	3.5759	2.7405
$\Delta \mathcal{L}_c$	0.0144	0.0045	0.0017	0.0007
Total	6.9400	4.8577	3.5776	2.7412
Expt.	6.9483(5)	4.8588(2)	3.5777(2)	2.7403(5)
$E-T$	0.0083(5)	0.0011(2)	0.0001(2)	-0.0009(5)
Standard atomic theory picture				
ΔE_{rel}	6.9301	4.8528	3.5753	...
$L1$	0.0129	0.0040	0.0015	...
$L2$	0.0048	0.0023	0.0012	...
Subtotal	6.9478	4.8590	3.5780	...
$\langle V_{\text{ret}}'' \rangle$	-0.0007	-0.0005	-0.0003	...
Total	6.9471	4.8585	3.5777	...
Expt.	6.9483(5)	4.8588(2)	3.5777(2)	2.7403(5)
$E-T$	0.0012(5)	0.0003(2)	0.0000(2)	...

and by Au and Mesa⁶ the SAT result implicitly includes the most significant part of $\langle V_{\text{ret}} \rangle$, namely, the expectation value of the first two terms in the short-range expansion⁵

$$V_{\text{ret}}(r) \cong \frac{\alpha^2}{Z^2} \left(\frac{a_0}{r} \right)^4 \left[1 - \frac{7}{6\pi} \left(Z^2 \alpha \frac{r}{a_0} \right) + \frac{1}{3} \left(Z^2 \alpha \frac{r}{a_0} \right)^2 + \dots \right] \frac{e^2}{a_0}$$

($r \leq 35a_0$), which appear as part of ΔE_{rel} and $L2$, respectively. The fact that this expansion converges poorly for $n=10$ Rydberg electrons (e.g., $-46.3+4.8-1.0+\dots$ kHz for the $G-H$ interval) suggests that the SAT approach could be in error at the kHz level. However, since the expectation value of the full function $V_{\text{ret}}(r)$ has been calculated for the states of interest,^{5,6} the difference between it and the contribution of the first two terms can be added as a correction $\langle V_{\text{ret}}'' \rangle$ to the SAT result, as shown in Table IV. This produces good agreement with experiment for the $I-K$ interval, but discrepancies of increasing significance at lower L . On the whole, agreement with experiment is not improved by including the $\langle V_{\text{ret}}'' \rangle$ correction. Whether these discrepancies can be explained within the SAT approach, perhaps by more careful treatment of the radiative shifts or by inclusion of the α^4 Rydberg terms, or whether they are related to the $\langle V_{\text{ret}}'' \rangle$ correction is an open question.

In summary, the precise measurements reported here

can be accounted for with fair but not total success by both the LRI and SAT pictures. In the LRI view the clear observation of the retardation effects $\langle V_{\text{ret}} \rangle$ realizes the suggestion of Kelsey and Spruch,¹ and the success of the LRI model encourages further studies at even larger r . The SAT calculation is even more successful in accounting for the measurements, but leaves a small discrepancy for the G - H interval whose explanation is not yet known. If this discrepancy proves to be related to the $\langle V_{\text{ret}} \rangle$ correction, its explanation would lie outside the framework of standard atomic structure theory. Additional precise measurements could continue to play an important role in the refinement of both approaches.

We thank Gordon Drake for communicating his theoretical results prior to publication. This work was supported by the National Science Foundation under Grant No. PHY87-09707.

^(a)Present address: Department of Physics, Occidental College, Los Angeles, CA 90041.

¹E. J. Kelsey and L. Spruch, Phys. Rev. A **18**, 15 (1978).

²R. J. Drachman, Phys. Rev. A **31**, 1253 (1985); **38**, 1659(E) (1988).

³G. W. F. Drake, J. Phys. B **22**, L651 (1989).

⁴C. K. Au, G. Feinberg, and J. Sucher, Phys. Rev. Lett. **53**, 1145 (1984); G. Feinberg, J. Sucher, and C. K. Au, Ann. Phys. (N.Y.) **173**, 355 (1987).

⁵J. F. Babb and L. Spruch, Phys. Rev. A **38**, 13 (1988).

⁶C. K. Au and M. A. Mesa, Phys. Rev. A **41**, 2848 (1990).

⁷S. L. Palfrey and S. R. Lundeen, Phys. Rev. Lett. **53**, 1141 (1984).

⁸E. A. Hessels, W. G. Sturuss, and S. R. Lundeen, Phys. Rev. A **35**, 4489 (1987).

⁹E. A. Hessels, W. G. Sturuss, and S. R. Lundeen, Phys. Rev. A **38**, 4574 (1988).

¹⁰E. A. Hessels, F. J. Deck, P. W. Arcuni, and S. R. Lundeen, Phys. Rev. A **41**, 3663 (1990).

¹¹The expected zero-field position of this resonance is obtained by extrapolating lower- n 3D - F transition frequencies calculated by G. W. F. Drake (private communication).

¹²J. W. Farley and W. H. Wing, Phys. Rev. A **23**, 2397 (1981).

¹³Based on hydrogenic lifetimes, the natural widths of the states studied are $\Gamma_G=88$, $\Gamma_H=58$, $\Gamma_I=41$, $\Gamma_K=31$, and $\Gamma_L=24$ kHz. The natural linewidth for the transition a to b is $\Gamma_a+\Gamma_b$, and this reflects the difficulty of the measurement, even though in a time-resolved measurement, such as this one, only the smaller width $\Gamma_a-\Gamma_b$ will contribute to the linewidth.

¹⁴G. W. F. Drake, following Letter, Phys. Rev. Lett. **65**, 2769 (1990).

¹⁵M. Martinis and H. Pilkuhn, J. Phys. B. **15**, 1797 (1982).

¹⁶D. R. Cok and S. R. Lundeen, Phys. Rev. A **19**, 1830 (1979); **24**, 3283(E) (1981).

¹⁷M. Idrees and C. F. Fischer, Nucl. Instrum. Methods Phys. Res., Sect. B **42**, 552 (1989).

¹⁸The results of Ref. 13 can be obtained by setting $a_1=1+a/\pi+2m/M$, $a_2=1+a/2\pi+m/M$, $a_3=1+a/\pi$ in Eq. (15) of Ref. 8. The values obtained using this prescription agree with Drake's values (Ref. 14) to better than 0.1 kHz for the $10I$ and $10K$ states, and should be accurate in predicting other high- L magnetic-fine-structure separations.

¹⁹R. J. Drachman, Phys. Rev. A **26**, 1228 (1982).

²⁰C. K. Au, G. Feinberg, and J. Sucher (private communication) have pointed out an oversight in the mass correction to this term. The coefficient $(1-2K)$ in Eq. (49) of Ref. 19 should be modified to read $(1-K/2)$ for the L -dependent term.

²¹References 4, 5, and 6 all give appropriate expectation values, but the numerical accuracy of Ref. 4 is apparently inferior to that of Refs. 5 and 6, which agree.